Acta Cryst. (1998). D**54**, 74–80

Melting Points of Lysozyme and Ribonuclease *A* Crystals Correlated with Protein Unfolding: a Raman Spectroscopic Study

J. Jacob,[a] C. Krafft,[b] K. Welfle,[b] H. Welfle[b] and W. Saenger[a]*

[a]*Institut für Kristallographie, Freie Universität Berlin, Takustrasse 6, D-14195 Berlin, Germany, and* [b]*Max-Delbrück-Centrum für Molekulare Medizin, Robert-Rössle-Strasse 10, D-13125 Berlin, Germany.*
E-mail: saenger@chemie.fu-berlin.de

(*Received 25 February 1997; accepted 28 July 1997*)

Abstract

The effects of a temperature increase on monoclinic and tetragonal lysozyme single crystals were investigated by polarizing microscopy, X-ray diffraction and laser Raman spectroscopy. To prevent dissolution, the mother liquor was removed, and the crystals were covered by the oil poly-(chlorotrifluoroethylene). Upon heating, their macroscopic shape was stable beyond 453 K but a change (or loss) of birefringence was observed around 352 and 367 K for the tetragonal and monoclinic crystal forms, respectively, which is associated with tighter packing and higher crystal forces in monoclinic lysozyme. Raman spectral changes in the amide I and amide III regions indicated denaturation of the protein within the crystalline environment at temperature where birefringence changes, and differences in the S—S band suggest that in monoclinic lysozyme, denaturation is accompanied with disruption of some S—S bonds. Comparison with thermal denaturation and gel formation (β-aggregation) of lysozyme in solution indicates that intermolecular interactions are mainly involved in the stabilization of the denatured lysozyme crystals. The behavior of ribonuclease *A* is very different. This protein unfolds and refolds reversibly in solution and its crystals melt at the unfolding temperature at 333 K, *i.e.* loss of structure induces breakdown of crystal lattice and macroscopic shape. Although the crystal lattice of proteins is stabilized by only few intermolecular contacts, its breakdown with increasing temperature is primarily a result of thermal unfolding of the polypeptide chains.

1. Introduction

For the assessment of purity and the characterization of crystalline organic compounds, it is common to determine their melting points. The melting point is associated with a cooperative sudden breakdown of the crystal lattice and represents a classical first-order phase transition.

Proteins are very large organic molecules. They consist of many thousands of atoms and are themselves regarded as macroscopic systems undergoing temperature-dependent phase transitions from the native folded to the denatured unfolded state (Privalov & Potekhin, 1986). In the native state, they can be crystallized if aqueous solutions of the proteins are supersaturated by addition of suitable precipitating agens. The crystals consist not only of protein but they also contain 30–80% mother liquor and can be considered as very concentrated solutions of fully hydrated proteins.

Since protein crystals are sensitive to X-ray radiation they are frequently cooled or even shock-frozen for crystallographic experiments (Parak *et al.*, 1987; Tilton *et al.*, 1992; Young *et al.*, 1994; Kurinov & Harrison, 1995). Here we address the question what happens if protein crystals are heated. In principle, two processes can take place, namely melting of the crystal lattice as known for organic crystals and/or thermal unfolding of the protein.

We have used crystals of hen egg-white lysozyme and of bovine pancreatic ribonuclease *A* for our studies. These proteins are commercially available, and their crystal structures are known in great detail (Blake *et al.*, 1965; Moult *et al.*, 1976; Hogle *et al.*, 1981; Artymiuk *et al.*, 1982; Hodson *et al.*, 1990; Ramanadham *et al.*, 1990; Borkakoti *et al.*, 1982). Lysozyme crystallizes in different forms (triclinic, monoclinic, orthorhombic and tetragonal) which is of additional interest in our studies.

The melting or breakdown of a crystal lattice can be directly observed by polarizing light microscopy or by X-ray diffraction. To monitor the possible unfolding of the proteins, we have used laser Raman spectroscopy, a method especially suited for this purpose as it can be conducted with proteins in crystalline form as well as in solution.

2. Experimental

2.1. *Materials*

Hen egg-white lysozyme (Grade VI) and ribonuclease *A* (type XII-A) were obtained from Sigma Chemical Company (Deisenhofen, Germany) and used without further purification. Monoclinic lysozyme crystals were grown according to published procedures (Hogle *et al.*, 1981; Artymiuk *et al.*, 1982; Young *et al.*, 1993) using the batch method. The final solution contained 1%

lysozyme, 2% $NaNO_3$ and 0.05 *M* sodium acetate buffer, pH 4.5; crystals appeared after 2 d at 291 K.

Tetragonal lysozyme crystals were grown using the vapor-diffusion technique. The reservoir contained 1.45 *M* NaCl, 0.05 *M* sodium acetate buffer, pH 4.5. Crystals grew at 291 K within 2 d from drops consisting of 3 µl of reservoir solution and 3 µl of 2% protein solution (0.05 *M* sodium acetate buffer, pH 4.5).

Crystals of ribonuclease *A* were grown at 291 K using the batch method from solutions containing 55% 2-methyl-2,4-pentanediol, 6% ribonuclease *A* and 0.05 *M* phosphate buffer, pH 6.5. Seeding was necessary to grow larger crystals.

If a protein crystal is heated in its mother liquor, it will dissolve smoothly. In order to observe the 'melting' behavior of the lysozyme and ribonuclease *A* crystals, mother liquor had to be removed and, to prevent drying, the crystals were covered with the mineral oil poly(chlorotrifluoroethylene) (Poflu). The oil has low viscosity and a relatively simple Raman spectrum which can be subtracted easily from the protein spectra.

2.2. *Optical microscopic observations*

The overall effects of temperature on crystals were observed by using an Olympus optical polarizing microscope to detect possible changes of birefringence. The heating experiments were carried out in the same way as described for the Raman measurements, using the same heating device and the same sample preparation.

2.3. *X-ray analysis*

The diffraction quality of both lysozyme crystal forms was checked with 3° angle precession photographs without preliminary orientation of the crystals. Crystals were mounted in glass capillaries and covered with Poflu. Capillaries were then fixed to a heating device from Enraf–Nonius. To check possible non-isomorphism of crystals protected with Poflu, the unit-cell parameters were measured at room temperature (293 K) using an Enraf–Nonius FAST area detector mounted on a FR571 rotating-anode X-ray generator.

2.4. *Laser Raman spectroscopy*

Raman spectra of single crystals were recorded by exciting at 488 nm with an Ar ion laser (Coherent Innova 90) using an Olympus BH2 microscope connected to a Jobin Yvon T64000 Raman spectrometer. The latter was equipped with a charge coupled device (CCD) detector cooled with liquid nitrogen and connected to a PC under Spectramax software. Typical experimental conditions were as follows: incident laser power, 150 mW with intensity of about 15 mW at the sample position; five accumulations of 30 s each. The wavenumber axis of the Raman spectra was calibrated with indene; peak positions were reproducible within 1 cm^{-1}. After subtraction of contributions from background, mother liquor and oil, all spectra were normalized to the methylene deformation mode at 1448 cm^{-1}.

A home-made device was used to regulate the sample temperature. It consists of an internal chamber (with two removable glass windows) which was connected to a type CH water bath and F3 temperature controller (Haake, Karlsruhe, Germany). For measurements, the upper window is replaced by a cover slip supporting the prepared crystal. This system permits a temperature accuracy at the sample position of ±2 K. Above 363 K, the inner chamber of the cell was heated electrically.

Because of anisotropy of single crystals of monoclinic and tetragonal space groups, Raman spectra are dependent on crystal orientation. Therefore, the same single crystal was measured with a fixed orientation during the whole experiment, so that band shifts and intensity changes are only related to structural and not to positional changes. For this reason, we cannot compare absolute changes between monoclinic and tetragonal crystal forms but only relative changes between spectra within the same data set.

To assess the error limits, several randomly orientated crystals were investigated by Raman spectroscopy. Only very little intensity effects were observed (2–5%) which confirms the validity of these qualitative analyses.

2.5. *Differential scanning calorimetry of lysozyme in solution*

Differential scanning calorimetric (DSC) measurements were performed using the precision scanning microcalorimeter DASM-4 (Institute of Protein Research Pushchino, Russia) as described earlier (Welfle *et al.*, 1996). The heating rate of 1 K min^{-1} was kept constant in all experiments. Lysozyme solutions were dialyzed against 0.5 *M* sodium acetate buffer, pH 4.5, containing 1.45, 1.0, 0.5 and 0.23 *M* sodium chloride, or 0.23 *M* sodium nitrate. The lysozyme concentrations were adjusted to about 2 mg ml^{-1} for the DSC measurements. Data analysis and deconvolution were performed using the standard software package *ORIGIN* supplied by *MICROCAL* Inc., Northampton, MA. The relative error of molar enthalpy changes ΔH is ± 4% and the absolute error of transition temperatures T_m is ± 0.3 K.

The ratio κ of the calorimetric and van't Hoff enthalpy changes ΔH^{cal} and ΔH^{vH} was calculated to judge the validity of the two-state mechanism for the unfolding of lysozyme.

3. Results

3.1. *Optical microscopic observations*

Preliminary information on the physical properties of the crystals was obtained from heating experiments carried out under an optical polarizing microscope.

Surprisingly, both monoclinic and tetragonal lysozyme crystals were stable at very high temperatures. Up to 453 K (temperature limit of the instrument), the macroscopic shape of the crystals did not change although the water contents of the tetragonal and monoclinic lysozyme crystals are 41 and 34%, respectively, and evaporation should occur.

As shown in Fig. 1 for the tetragonal crystal form of lysozyme, the temperature increase is accompanied by a change of birefringence; a similar yet less pronounced effect has also been observed with monoclinic lysozyme crystals. Changes of birefringence were observed around 353 and 368 K for tetragonal and monoclinic crystal forms, respectively, indicating a higher thermal stability of the latter. For some crystals, the birefringence even disappeared completely, indicating that they become optically isotropic in the observed direction. The reduction or loss of birefringence is irreversible and remains after cooling the crystal to ambient temperature as shown by Fig 1(*d*).

The same experiment was carried out with crystals of ribonuclease *A*, which is one of the proteins that do not aggregate upon thermal denaturation in solution but refold reversibly after cooling (Beck *et al.*, 1965). At approximately 333 K, close to the unfolding temperature of the protein in solution (335 K; Tsong *et al.*, 1970), crystals cracked and slowly 'melted' in the surrounding oil and formed drops. This is in striking contrast to lysozyme crystals which maintain their macroscopic shape even at 453 K.

3.2. *X-ray analysis*

Precession photographs confirmed the temperature stability of the lysozyme crystals which were still diffracting at 333 K. At higher temperatures, the diffraction decreased and finally disappeared around 353 K. Unfortunately, a more accurate study was impossible due to increase of mosaic spread causing reflections to become broader, weaker and more diffuse. When the crystals were cooled to room temperature, the diffraction pattern did not reappear indicating that similar to the loss of birefringance, the phenomenon is irreversible once the diffraction or birefringance have been reduced by temperature effects.

3.3. *Laser Raman spectroscopy*

In agreement with the observations reported above, no Raman spectral changes were observed up to 348 and 358 K for the lysozyme tetragonal and monoclinic crystal forms respectively. This means that no major structural changes occurred in this temperature range. Heating of the crystals to higher temperatures was accompanied by irreversible changes in the spectra (see Figs. 2 and 3). By comparison with Raman spectroscopic studies reported earlier on the thermal denaturation of lysozyme in solution (Brunner & Sussner, 1972; Chen *et al.*, 1973; Porubcan *et al.*, 1978), the spectral changes observed in both crystal forms can be assigned to denaturation of the protein within the crystalline environment. In Table 1, the band maxima of the native and denatured tetragonal and monoclinic crystal forms are summarized.

After heating, the most evident changes for lysozyme in both crystal forms and in solution (not shown; see

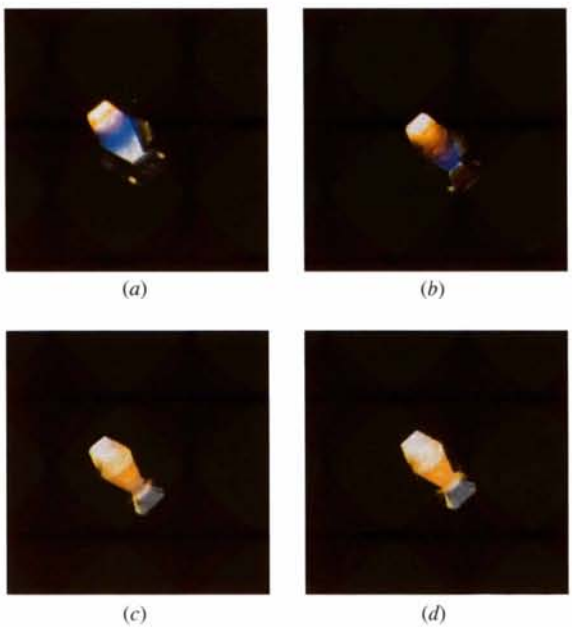

Fig. 1. Birefringence changes in tetragonal lysozyme crystal upon temperature increase [a = 296, b = 353, c = 393 K; d = cooled to room temperature (293 K)].

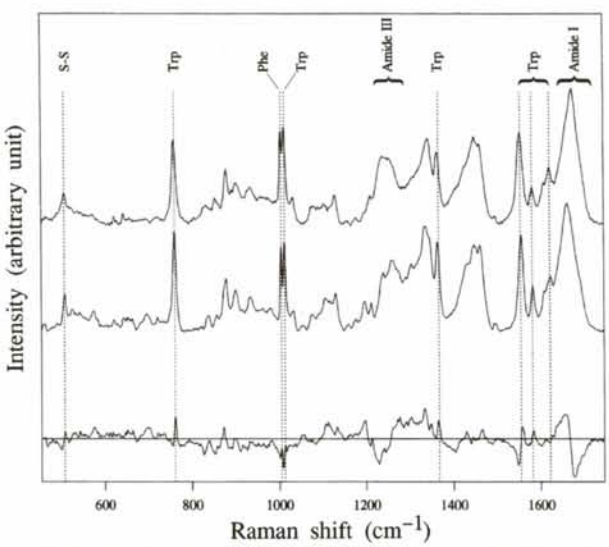

Fig. 2. Raman spectra of a tetragonal lysozyme single crystal in the denatured state (top spectrum, T = 358 K) and in the native state (middle spectrum, T = 296 K) after subtraction of contributions due to background, mother liquor and oil. The bottom spectrum is the difference between the spectra of native and denatured lysozyme.

Table 1. *Band maxima observed for lysozyme tetragonal and monoclinic single crystals (all data in cm^{-1})*

Tetragonal		Monoclinic		Tentative assignment
Native	Denatured	Native	Denatured	
507	506	507	506	ν(S—S)†
760	758	759	759	Trp
838	832	838	832	Tyr
856	854	857	856	Tyr
878	878	878	878	Trp
899	900	901	903	ν(C—C)
933	933	933	933	ν(C—C)
1004	1004	1004	1004	Phe
1012	1012	1012	1012	Trp
1032	1032	1033	1032	Phe
1076	1077	1077	—	ν(C—N)
1102	1106	1106	1105	ν(C—N)
1129	1128	1130	1129	ν(C—C)
1177	1177	—	—	Tyr
1196	—	1197	—	Tyr
1211	1210	1211	1211	Tyr, Phe
1238		1237		Amide III
1258	1245	1249	1246	Amide III
1273		1273		Amide III
1335	1341	1336	1341	Trp and CH deformation
1363	1361	1362	1362	Trp and CH deformation
1448	1448	1448	1448	CH_2 deformation
1459	1459	1460	1460	CH_2 deformation
1555	1553	1555	1553	Trp
1581	1580	1581	1581	Trp
1622	1621	1621	1621	Trp, Tyr and Phe
1661	1672	1659	1672	Amide I

† Stretching vibration.

Brunner & Sussner, 1972; Chen *et al.*, 1973) include the following (Figs. 2 and 3, Table 1): (1) a shift of the amide I band to higher wavenumbers, (2) a shift of the amide III band which is centered after denaturation around 1245 cm^{-1}, and (3) a decrease in the intensity of the peaks at ~760, 878, 1363 and 1553 cm^{-1}.

In protein vibrational spectroscopy, the amide I and III bands are sensitive to the conformation of the polypeptide main chain and have been extensively used for secondary-structure determination (for review, see Krimm & Bandekar, 1986; Fabian & Anzenbacher, 1993; Peticolas, 1995). The changes observed for these two bands in lysozyme crystals can be related to a decrease of the α-helical content accompanied by an increase of the β-sheet and random coil structure. To determine the melting points of the protein in the two different crystalline states, the position of the amide I band *versus* the temperature has been plotted in Fig. 4. As observed with the birefringence, monoclinic lysozyme crystals melt 15 K higher (367 K), than the tetragonal ones (352 K), indicating a higher thermal stability.

Other significant changes occur in various characteristic Raman frequencies of the amino-acid side chains. Intensities and half-band widths assigned to tryptophan are sensitive to the microenvironment and to the conformation of tryptophan residues. The general decrease of intensity of the concerned bands upon heating indicates increased exposure of tryptophan residues to the aqueous environment. Especially, the intensity decrease of the 1363 cm^{-1} peak of the Trp doublet around 1334–1363 cm^{-1} suggests that some of the tryptophans were initially in hydrophobic regions in native lysozyme and are in a more hydrophilic environment after denaturation (Harada *et al.*, 1986). According to X-ray structure analysis, Trp28 and Trp111 are located in the hydrophobic core of lysozyme, and changes in their environment could give rise to the observed spectral differences.

Although the spectral changes with temperature are comparable for monoclinic and tetragonal crystals of

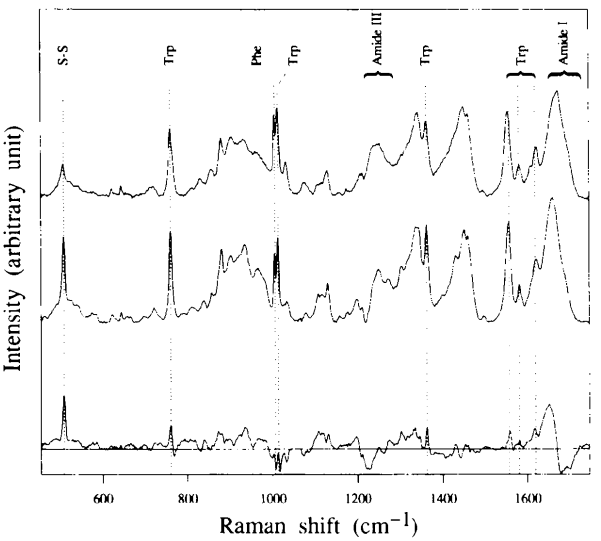

Fig. 3. Raman spectra of monoclinic lysozyme single crystal in the denatured state (top spectrum, T - 371 K) and in the native state (middle spectrum, T = 296 K) after subtraction of contributions due to background, mother liquor and oil. The bottom spectrum is the difference between the spectra of native and denatured lysozyme.

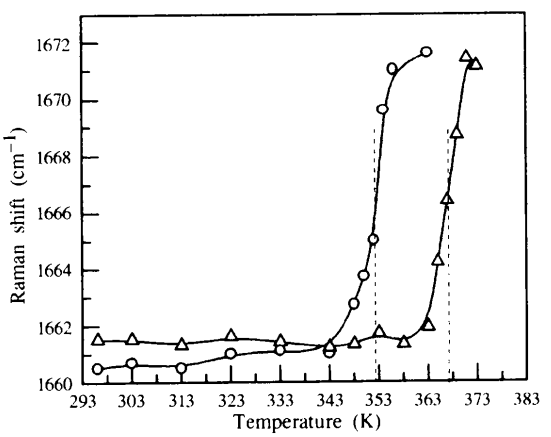

Fig. 4. Amide I band position *versus* temperature for tetragonal (open circles) and monoclinic (open triangles) single crystal of lysozyme. The dashed lines represent the melting temperatures (T_m) at 352 and 367 K, respectively.

lysozyme, there are significant differences between the two crystal forms.

As shown by the difference spectra (bottom spectra of Figs. 2 and 3), the major difference is related to the characteristic frequency of the disulfide bridges (around 507 cm^{-1}). In tetragonal lysozyme, the peak intensity decreased only slightly which means that the number of disulfide bridges does not seem to be affected. On the contrary, the high positive 507 cm^{-1} peak of the difference spectrum of the monoclinic crystal indicates that the number of S—S bridges is reduced. Unfortunately, the C—S stretching band around 660 cm^{-1} [which is sensitive for the geometry of the C—S—S—C group (Lord & Yu, 1970)] is hidden by a strong component of Poflu which impedes further investigations.

The tryptophan band around 1550 cm^{-1} shows also a different behavior depending on the crystal form. It usually serves as marker for the orientation of the indole ring with respect to the peptide backbone (Miura *et al.*, 1989). For the monoclinic crystals, thermal denaturation gives rise to a decrease of intensity while for the tetragonal ones, this intensity decrease is accompanied by a small blue shift (see Table 1). This can be interpreted by larger changes in the environment of tryptophan residues when tetragonal lysozyme crystals melt.

A closer look at the amide I band region of the difference spectra also indicates a different behavior of the two lysozyme crystal forms. In the difference spectrum of the tetragonal lysozyme crystals, the negative lobe of the amide band is more intense than the positive one while the opposite is observed in the difference spectrum of the monoclinic form. This indicates that in tetragonal crystals, larger secondary-structure changes have occurred than in monoclinic crystals.

In contrast to the high thermal stability of the macroscopic shape of lysozyme crystals, ribonuclease *A* crystals cracked and melted at approximately 333 K, forming drops. By comparison with Raman spectroscopic studies reported earlier on the thermal denaturation of ribonuclease *A* in solution (Chen & Lord, 1976) and in the crystalline state (Gilbert *et al.*, 1982), the intensity increase of the 1250 cm^{-1} component of the amide III band with higher temperature and other spectral changes were assigned to denaturation of the protein.

3.4. *DSC calorimetry of lysozyme in solution*

Since tetragonal and monoclinic crystal forms of lysozyme were grown at the same pH (0.05 *M* sodium acetate buffer, pH 4.5) but different kind and concentration of salts (1.45 *M* NaCl and 0.23 *M* $NaNO_3$, respectively), it was of interest to investigate the thermal unfolding of lysozyme under these conditions in solution, without the influence of the crystal lattice. Fig. 3 shows the excess heat capacity curves of lysozyme in 0.05 *M* sodium acetate buffer, pH 4.5, containing 1.4 *M* sodium chloride (*A*) and 0.23 *M* $NaNO_3$ (*B*). Also, melting temperatures T_m and molar enthalpy changes ΔH_m were determined in buffer containing 0.23, 0.5 and 1.0 *M* NaCl (Table 2).

Table 2. *Melting temperatures and enthalpy changes of lysozyme in solution measured by differential scanning calorimetry*

All solutions contained 0.05 *M* sodium acetate buffer, pH 4.5. Protein concentrations varied from 1.4 to 2.0 mg ml^{-1}. NaCl and $NaNO_3$ concentrations which were used in the crystallization experiments are given in italics.

Salt	Salt concentration (*M*)	T_m (K)	ΔH_m (kJ mol^{-1})†
NaCl	*1.45*	350.5	452
	1.00	350.2	443
	0.50	350.1	477
	0.23	350.0	481
$NaNO_3$	*0.23*	348.3	456

† 1 kcal mol^{-1} = 4.184 kJ mol^{-1}.

T_m and ΔH_m values of lysozyme are similar for all studied conditions. The stability of lysozyme in solution is practically independent of the NaCl concentration, and the changes to 0.23 *M* $NaNO_3$ has only a minor effect. The excess heat capacity curves clearly indicate a two-state transition of lysozyme for all tested conditions as well known for hen egg-white lysozyme (Griko *et al.*, 1995).

4. Discussion

In both tetragonal and monoclinic crystal forms of lysozyme and in crystals of ribonuclease *A*, the temperature dependence of the birefringence indicated structural changes induced by increased temperatures. Since the X-ray diffraction disappeared above 343 K, laser Raman spectroscopy was applied to study this phenomenon. Changes in the amide I and amide III regions could be assigned to a thermal denaturation of the two proteins.

In solution at suitable conditions, the thermal denaturation of lysozyme, and many other proteins, is accompanied with gel formation (Shimada & Matsushita, 1980; Ma & Holme, 1982; Gossett *et al.*, 1984). It has been suggested that noncovalent interactions, predominantly of hydrophobic and hydrogen-bonding type, lead to the formation of β-pleated sheet structures (β-aggregation), which give rise to and stabilize the gel network (Shimada & Matsushita, 1981; Hayakawa & Nakamura, 1986; Li-Chan & Nakai, 1991; Przbycien & Bailey, 1991). Li-Chan & Nakai (1991) have used laser Raman spectroscopy to investigate the thermal formation of lysozyme gels in the presence or absence of dithiothreitol. They concluded that the energy for

unfolding is supplied by the increase in temperature and allows exposure of previously buried hydrophobic groups, conformational rearrangement and realignment of molecular segments, including probably the formation of intermolecular β-sheets structures. Since the spectral changes observed here with crystalline lysozyme are nearly identical to those reported earlier for gelation in solution, we assume that they also indicate denaturation followed by β-aggregation which 'cross-links' the molecules in the crystal lattice. This is supported by the observation that after denaturation, it was impossible to redissolve lysozyme crystals, suggesting intermolecular hydrophobic and/or hydrogen-bonding 'cross-linking' of the crystals by the gel network. We assume that the network also maintains the water content of the crystals, *i.e.* even well above 373 K water or water bubbles do not emerge from the crystals.

Crystals of ribonuclease *A* crack and melt at approximately 333 K, in striking contrast to lysozyme crystals. Using laser Raman spectroscopy, it has been shown that cracking of ribonuclease *A* crystals is accompanied by thermal denaturation of the protein but not by intermolecular aggregation as in the case of lysozyme. The analysis of the crystal structure of ribonuclease *A* revealed that the overall three-dimensional structure does not change significantly in the range 98–320 K (Tilton *et al.*, 1992). Gilbert *et al.* (1982) studied temperature dependent conformational changes of crystalline ribonuclease *A* by X-ray diffraction and Raman spectroscopy, and reported denaturation of crystalline ribonuclease *A* occurring at about 333 K, as confirmed by our data. The main difference between the Raman experiments is that Gilbert *et al.* investigated polycrystalline material to avoid anisotropy problems while we took the spectra from single crystals using an optical microscope.

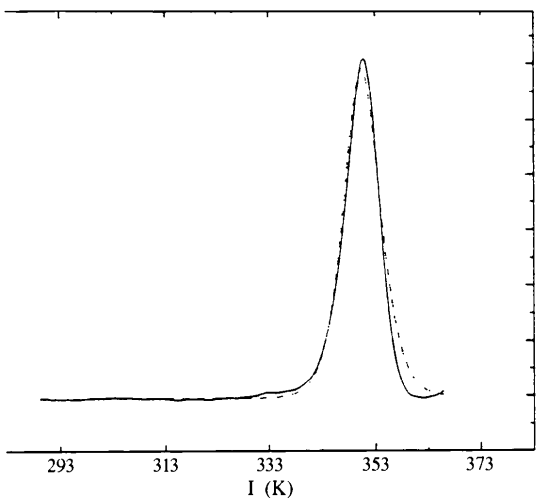

Fig. 5. Deconvolution of excess heat capacity functions of lysozyme (solid line: experimental data, dashed line: theoretical fit). The sample was dialyzed against 0.05 *M* sodium acetate buffer, pH 4.5, containing 1.45 *M* NaCl at protein concentration of 2 mg ml^{-1}. Melting points T_m (K) and ΔH_m (kJ mol^{-1}) are reported in Table 2. For all solutions described in Table 2, similar experimental and theoretical curves were obtained.

Monoclinic and tetragonal crystal forms of lysozyme differ in packing arrangement and in the order of water molecules. The monoclinic form is tighter packed than the tetragonal form, with 1.83 and 2.04 Å^3 occupied per Dalton of protein, respectively. At 1.9 Å resolution, 191 water molecules were located in the asymmetric unit of the monoclinic form but only 100 in that of the tetragonal form. This indicates that the monoclinic crystal form seems to be structurally better defined accompanied by a higher thermal stability in comparison to the tetragonal form, as indeed observed.

DSC data (Table 2, Fig. 5) show that the different conditions necessary to obtain tetragonal and monoclinic lysozyme crystals do not strongly affect the thermal stability of the protein. This indicates that the melting points of lysozyme crystals strongly depend on the crystal packing. Thus, qualitative information on crystal packing forces can be obtained studying the melting of protein crystals.

This work was supported by a grant from the EU program Human Capital and Mobility, by the *DFG-Sonderforschungsbereich* 344, by *DFG-Graduiertenkolleg Modellstudien zur Struktur und Erkennung biologischer Moleküle auf atomarer Ebene*, and by *Fonds der Chemischen Industrie*.

References

Artymiuk, P. J., Blake, C. C. F., Rice, D. W. & Wilson, K. S. (1982). *Acta Cryst.* B**38**, 778–783.

Beck, K., Gill, S. J. & Downing, M. (1965). *J. Am. Chem. Soc.* **87**, 901–903.

Blake, C. C. F., Koenig, D. F., Mair, G. A., North, A. C. T., Phillips, D. C. & Sarma, V. R. (1965). *Nature (London)*, **206**, 757–761.

Borkakoti, N., Moss, D. S. & Palmer, R.A. (1982). *Acta Cryst.* B**38**, 2210–2217.

Brunner, H. & Sussner, H. (1972). *Biochim. Biophys. Acta*, **271**, 16–22.

Chen, M. C. & Lord, R. C. (1976). *Biochemistry*, **15**, 1889–1897.

Chen, M. C., Lord, R. C. & Mendelsohn, R. (1973). *Biochim. Biophys. Acta*, **328**, 252–260.

Fabian, H. & Anzenbacher, P. (1993). *Vib. Spectrosc.* **4**, 125–148.

Gilbert, W. A., Lord, R. C., Petsko, G. A. & Thamann, T. J. (1982). *J. Raman Spectrosc.* **12**, 173–179.

Gossett, P. W., Rizvi, S. S. H. & Baker, R. C. (1984). *Food Technol.* **38**, 67–96.

Griko, Y. V., Freire, E., Privalov, G., van Dael, H. & Privalov, P. L. (1995). *J. Mol. Biol.* **254**, 447–459.

Harada, I., Miura, T. & Takeuchi, H. (1986). *Spectrochim. Acta*, **42**, 307–312.

Hayakawa, S. & Nakamura, R. (1986). *Agric. Biol. Chem.* **50**, 2039–2046.

Hodson, J. M., Brown, G. M., Sieker, L. C. & Jensen, L. H. (1990). *Acta Cryst.* B**46**, 54–62.

Hogle, J., Rao, S. T., Mallikarjunan, M., Bedsell, C., McMullan, R. K. & Sundaralingam, M. (1981). *Acta Cryst.* B**37**, 591–597.

Krimm, S. & Bandekar, J. (1986). *Adv. Prot. Chem.* **38**, 181–364.

Kurinov, I. V. & Harrison, R. W. (1995). *Acta Cryst.* D**51**, 98–109.

Li-Chan, E. & Nakai, S. (1991). *J. Agric. Food Chem.* **39**, 1238–1245.

Lord, R. C. & Yu, N. T. (1970). *J. Mol. Biol.* **50**, 509–524.

Ma, C. Y. & Holme, J. (1982). *J. Food Sci.* **47**, 1454–1459.

Miura, T., Takeuchi, H. & Harada, I. (1989). *J. Raman Spectrosc.* **20**, 667–671.

Moult, J., Yonath, A., Traub, W., Smilansky, A., Podjarny, A., Rabinovich, D. & Saya, A. (1976). *J. Mol. Biol.* **100**, 179–195.

Parak, F., Hartmann, H., Aumann, K. D., Reuscher, H., Rennekamp, G., Bartunik, H. & Steigemann, W. (1987). *Eur. Biophys. J.* **15**, 237–249.

Peticolas, W. L. (1995). *Methods Enzymol.* **246**, 389–416.

Porubcan, R. S., Watters, K. L. & McFarland, J. T. (1978). *Arch. Biochem. Biophys.* **186**, 255–264.

Privalov, P. L. & Potekhin, S. A. (1986). *Methods Enzymol.* **131**, 4–51.

Przybycien, T. M. & Bailey, J. E. (1991). *Biophys. Acta*, **1076**, 103–111.

Ramanadham, M., Sieker, L. C. & Jensen, L. H. (1990). *Acta Cryst.* B**46**, 63–69.

Shimada, K. & Matsushita, S. (1980). *J. Agric. Food Chem.* **28**, 413–417.

Shimada, K. & Matsushita, S. (1981). *J. Agric. Food Chem.* **29**, 15–20.

Tilton, R. F., Dewan, J. C. & Petsko, G. A. (1992). *Biochemistry*, **31**, 2469–2481.

Tsong, T. Y., Hearn, R. P., Wrathall, D. P. & Sturtevant, J. M. (1970). *Biochemistry*, **9**, 2666–2677.

Welfle, K., Misselwitz, R., Politz, O., Borriss, R. & Welfle, H. (1996). *Protein Sci.* **5**, 2255–2265.

Young, A. C. M., Dewan, J. C., Nave, C. & Tilton, R. F. (1993). *J. Appl. Cryst.* **26**, 309–319.

Young, A. C. M., Tilton, R. F. & Dewan, J. C. (1994). *J. Mol. Biol.* **235**, 302–317.